Semiempirical atomic potentials for the fcc metals Cu, Ag, Au, Ni, Pd, Pt, Al, and Pb based on first and second nearest-neighbor modified embedded atom method

Byeong-Joo Lee,[1,*] Jae-Hyeok Shim,[2] and M. I. Baskes[3,†]
[1]*Department of Materials Science and Engineering, Pohang University of Science and Technology, Pohang 790-784, Republic of Korea*
[2]*Materials Science and Technology Division, Korea Institute of Science and Technology, Seoul 136-791, Republic of Korea*
[3]*Structure/Properties Relation Group, Los Alamos National Laboratory, MS G755, Los Alamos, New Mexico 87545, USA*
(Received 17 February 2003; published 29 October 2003)

Modified embedded atom method (MEAM) potentials for fcc elements Cu, Ag, Au, Ni, Pd, Pt, Al, and Pb have been newly developed using the original first nearest-neighbor MEAM and the recently developed second nearest-neighbor MEAM formalisms. It was found that the original MEAM potentials for fcc elements show some critical shortcomings such as structural instability and incorrect surface reconstructions on (100), (110), and/or (111) surfaces. The newly developed MEAM potentials solve most of the problems and describe the bulk properties (elastic constants, structural energy differences), point defect properties (vacancy and interstitial formation energy and formation volume, activation energy of vacancy diffusion), planar defect properties (stacking fault energy, surface energy, surface relaxation and reconstruction), and thermal properties (thermal expansion coefficients, specific heat, melting point, heat of melting) of the fcc elements considered, in good agreement with relevant experimental information. It has been shown that in the MEAM the degree of many-body screening (C_{min}) is an important material property and that structural stability at finite temperatures should be included as a checkpoint during development of semiempirical potentials.

DOI: 10.1103/PhysRevB.68.144112 PACS number(s): 61.50.Lt, 62.20.Dc, 64.70.Dv, 64.70.Kb

I. INTRODUCTION

By helping to interpret experiments, find governing rules, and predict materials properties, computational approaches are becoming more and more powerful tools in materials science and engineering society. Especially, atomistic simulations (molecular dynamics or Monte Carlo simulations) based on semiempirical atomic potentials, which can now cover over millions of atoms, are being applied to study polycrystalline bulk properties of real materials as well as surface or point defect properties. The application of the atomistic approach is not confined to pure elements but is being extended to multicomponent alloy systems.

The essence of the semiempirical approach is that the atomic potentials should be able to describe the fundamental physical properties of the real elements or alloy systems under consideration. Several atomic potential models have been developed and are used. However, most of them are for specific elements—for example, only for fcc elements, only for bcc elements, or only for diamond structured elements. Therefore, the alloy systems that can be covered are mostly those composed of elements of the same crystal structures. In order to apply the atomistic approach to wider range of alloy systems it is important to be able to describe wide range of elements with various crystal structures using a common formalism.

The modified embedded atom method (MEAM) potential proposed by Baskes *et al.*[1–4] was the first semiempirical atomic potential formalism that showed the possibility that one single formalism can be applied to a wide range of elements including fcc, bcc, hcp, diamond-structured elements, and even gaseous elements. However, the originally published MEAM parameter sets[3,4] showed some critical shortcomings. For example, in the case of bcc elements, the bcc structure was not the most stable structure and other structures were created during molecular dynamics (MD) runs at finite temperatures.

It was thought that the problem of the MEAM in the description of bcc elements originates from the fact that the original MEAM considers only first nearest-neighbor interactions but not second nearest-neighbor interactions whose distance is larger than the first nearest-neighbor distance by only 15%. The MEAM formalism was modified once again so that it can consider the second nearest-neighbor interactions partially. Using this new MEAM formalism which was named the second nearest-neighbor MEAM (2NN MEAM),[5,6] the problems found in the original first nearest-neighbor MEAM (1NN MEAM) for bcc elements could be solved.

However, recently, a similar problem on the structural stability was found by Mae *et al.*[7] in the MEAM potentials for hcp elements. They reported that among the 18 hcp elements described by the MEAM (Ref. 4) only 7 stay in the hcp structure after MD runs at a finite temperature while others result in a stable structure different from the hcp.

The present authors thought that the above problems of the 1NN MEAM for bcc and hcp elements were caused because the model parameters were determined by some mechanical procedures based on 0 K physical properties without considering the relaxations or probable reconstructions at finite temperatures. Then, the present authors decided to carefully examine the structural stabilities of fcc elements by MEAM at finite temperatures. Because fcc elements were the representative elements which could be successfully described by many other empirical atomic potential models, it was expected that the MEAM would not result in any critical shortcomings for fcc elements. Unfortunately, however, some critical shortcomings were also found in the MEAM potentials[3] for fcc elements.

The present authors examined the MEAM potentials on Cu, Ag, Au, Ni, Pd, Pt, Al, and Pb. Three different problems were found in the MEAM descriptions[3] on the above eight fcc elements. First, for Al, the fcc structure was not the most stable structure. A hexagonal structure whose potential energy is much more negative than that of fcc was created during MD runs at a finite temperature. Second, unexpected surface reconstructions or even structural transitions were found when a finite-temperature MD run was performed on thin films with a (100), (110), or (111) surface. Third, in general, the MEAM potentials for the fcc elements resulted in too low thermal expansion coefficients in comparison with experimental information. The calculated values of thermal expansion coefficients of fcc elements at the temperature range of 0–100 °C were lower than experimental data by about one order of magnitude. During the present work, it was found that most of the above problems in the MEAM potentials of fcc elements could be solved by redetermining the model parameters, paying special attention to the degree of many-body screening as has been done in the development of the 2NN MEAM.[5,6]

The purpose of the present work is to provide new (1NN or 2NN) MEAM parameter sets for the fcc elements Cu, Ag, Au, Ni, Pd, Pt, Al, and Pb, which does not result in the above-mentioned unexpected structural transitions or unexpected surface reconstructions and result in good agreement with experimental information in the thermal expansion coefficient as well as other physical properties that could readily be described satisfactorily. In Sec. II, the formalism of the MEAM will be briefly described. Here, the difference between the original 1NN MEAM and the 2NN MEAM will be highlighted. In Sec. III, the procedure for the determination of parameter values will be given. Comparisons between some calculated and experimental physical properties of the fcc elements will be given in Sec. IV. The general performance of the present potentials and the importance of the degree of many-body screening as a material property in MEAM will also be discussed in this section, and Sec. V is a summary.

II. FORMALISM

A full description on the original MEAM formalism has been published in the literature[3,4] and the formalism of the 2NN MEAM has also been published in detail.[6] In this section, both models will be briefly reviewed highlighting the commonness and difference between them.

A. MEAM

In the MEAM, the total energy of a unary system is approximated as

$$E=\sum_i \left[F(\overline{\rho}_i)+\frac{1}{2}\sum_{j(\neq i)} \phi(R_{ij}) \right]. \tag{1}$$

F is the embedding function, $\overline{\rho}_i$ is the background electron density at site i, and $\phi(R_{ij})$ is the pair interaction between atoms i and j separated by a distance R_{ij}. The embedding function is given as follows:

$$F(\overline{\rho})=AE_c(\overline{\rho}/\overline{\rho}^0)\ln(\overline{\rho}/\overline{\rho}^0). \tag{2}$$

Here, A is an adjustable parameter, E_c is the sublimation energy, and $\overline{\rho}^0$ is the background electron density for a reference structure. The reference structure is a structure where individual atoms are on the exact lattice points without deviation. Normally, the equilibrium structure is taken as the reference structure for elements. The background electron density $\overline{\rho}_i$ is composed of a spherically symmetric partial electron density $\rho_i^{(0)}$ and the angular contributions $\rho_i^{(1)}$, $\rho_i^{(2)}$, and $\rho_i^{(3)}$. Each partial electron density term has the following form:

$$(\rho_i^{(0)})^2=\left[\sum_{j\neq i} \rho_j^{a(0)}(R_{ij})\right]^2, \tag{3a}$$

$$(\rho_i^{(1)})^2=\sum_\alpha \left[\sum_{j\neq i} \frac{R_{ij}^\alpha}{R_{ij}}\rho_j^{a(1)}(R_{ij})\right]^2, \tag{3b}$$

$$(\rho_i^{(2)})^2=\sum_{\alpha,\beta}\left[\sum_{j\neq i} \frac{R_{ij}^\alpha R_{ij}^\beta}{R_{ij}^2}\rho_j^{a(2)}(R_{ij})\right]^2-\frac{1}{3}\left[\sum_{j\neq i}\rho_j^{a(2)}(R_{ij})\right]^2, \tag{3c}$$

$$(\rho_i^{(3)})^2=\sum_{\alpha,\beta,\gamma}\left[\sum_{j\neq i} \frac{R_{ij}^\alpha R_{ij}^\beta R_{ij}^\gamma}{R_{ij}^3}\rho_j^{a(3)}(R_{ij})\right]^2 -\frac{3}{5}\sum_\alpha\left[\sum_{j\neq i}\frac{R_{ij}^\alpha}{R_{ij}}\rho_j^{a(3)}(R_{ij})\right]^2. \tag{3d}$$

Here, $\rho_j^{a(h)}$ represent atomic electron densities from j atom at a distance R_{ij} from atom i. R_{ij}^α is the α component of the distance vector between atoms j and i ($\alpha=x,y,z$). The expression for $(\rho_i^{(3)})^2$ [Eq. (3d)] is a recent modification to make the partial electron densities orthogonal.[8] The way of combining the partial electron densities to give the total background electron density is not unique, and several expressions have been proposed.[9] Among them, the following form is used in the present work:

$$\overline{\rho}_i=\rho_i^{(0)}\cdot 2/(1+e^{-\Gamma_i}), \tag{4}$$

where

$$\Gamma_i=\sum_{h=1}^{3} t^{(h)}[\rho_i^{(h)}/\rho_i^{(0)}]^2 \tag{5}$$

and $t^{(h)}$ are adjustable parameters. The atomic electron density is given as

$$\rho^{a(h)}(R)=e^{-\beta^{(h)}(R/r_e-1)}, \tag{6}$$

where $\beta^{(h)}$ are adjustable parameters and r_e is the nearest-neighbor distance in the equilibrium reference structure.

Using Eqs. (3)–(6), the background electron density at each atomic site can be computed both for a given reference structure without thermal deviation of individual atoms and for a general atomic configuration with thermal deviation of atoms. Then the embedding function values can be computed

for individual atoms according to Eq. (2). Now, for the energy calculation the pair interaction terms in Eq. (1) should be computed. In the MEAM, no specific functional expression is given directly to $\phi(R)$. Instead, the energy per atom for the equilibrium reference structure is given a value as a function of atomic volume (nearest-neighbor distance). Then, the value of $\phi(R)$ is computed from the known values of the total energy per atom and the embedding function, as a function of nearest-neighbor distance R.

The value of the energy per atom for the equilibrium reference structure is obtained from the zero-temperature universal equation of state by Rose *et al.*[10] as a function of nearest-neighbor distance R:

$$E^u(R) = -E_c(1+a^*+da^{*3})e^{-a^*}, \tag{7}$$

where d is an adjustable parameter and

$$a^* = \alpha(R/r_e - 1) \tag{8}$$

and

$$\alpha = (9B\Omega/E_c)^{1/2}. \tag{9}$$

$E^u(R)$ is the universal function for a uniform expansion or contraction in the reference structure, r_e is the equilibrium nearest neighbor distance, B is the bulk modulus, and Ω is the equilibrium atomic volume.

Here, it should be noted that for a given reference structure where bonding directions among neighbor atoms are fixed, the embedding function and the energy per atom becomes a function of only nearest-neighbor distance. If only first nearest-neighbor interactions are considered as in the original 1NN MEAM, the energy per atom can be written as follows:

$$E^u(R) = F[\overline{\rho}^0(R)] + (Z_1/2)\phi(R), \tag{10}$$

where Z_1 is the number of nearest-neighbor atoms. The expressions for the embedding function F and energy per atom $E^u(R)$ are now available [from Eqs. (2) and (7), respectively]. The expression for the pair interaction between two atoms separated by a distance R, $\phi(R)$, is obtained from Eq. (10) as follows:

$$\phi(R) = (2/Z_1)\{E^u(R) - F[\overline{\rho}^0(R)]\}. \tag{11}$$

B. Difference between the 1NN MEAM and the 2NN MEAM

The key difference between the 1NN and 2NN MEAM is that second nearest-neighbor interactions are considered in the 2NN MEAM. In the 2NN MEAM, the summations in Eqs. (3a)–(3d) for computation of partial electron densities are extended to the second nearest-neighbor atoms. The same extension is made also in the summation for computation of pair interactions in Eq. (1). Therefore, the equation for energy per atom [Eq. (10)] should be also modified so that it involves the pair interactions with second nearest-neighbor atoms as follows:

$$E^u(R) = F[\overline{\rho}^0(R)] + (Z_1/2)\phi(R) + (Z_2S/2)\phi(aR). \tag{12}$$

Here, Z_2 is the number of second nearest-neighbor atoms, and a is the ratio between the second and first nearest-neighbor distances. S is the screening function on the second nearest-neighbor interactions and will be described in more detail at the end of this section. It will only be mentioned here that the screening function S is a material constant in the 2NN MEAM. By introducing another pair potential $\psi(R)$, Eq. (12) can be written again as follows:

$$E^u(R) = F[\overline{\rho}^0(R)] + (Z_1/2)\psi(R), \tag{13}$$

where

$$\psi(R) = \phi(R) + (Z_2S/Z_1)\phi(aR). \tag{14}$$

Now, $\psi(R)$ can be calculated from Eq. (13) as a function of R. Then, the pair potential $\phi(R)$ is calculated using the following relation, also as a function of R:

$$\phi(R) = \psi(R) + \sum_{n=1} (-1)^n (Z_2S/Z_1)^n \psi(a^nR). \tag{15}$$

Here, the summation is performed until the correct value of energy is obtained for the equilibrium reference structure.

It has been mentioned that only first nearest-neighbor interactions are considered in the 1NN MEAM. The neglect of the second nearest-neighbor interactions is made by the use of a strong many-body screening function. In the same way, the consideration of the second nearest-neighbor interactions in the 2NN MEAM is also made by adjusting the many-body screening function so that it becomes less severe.

The amount of screening of a k atom to the interaction between i and j atoms is determined using a simple geometric construction.[9,11] Imagine an ellipse on an x, y plane, passing through atoms i, k, and j, with the x axis of the ellipse determined by atoms i and j. The equation of the ellipse is given by

$$x^2 + (1/C)y^2 = \left(\frac{1}{2}R_{ij}\right)^2. \tag{16}$$

For each k atom, the C value can be computed from the relative distances among the three atoms i, j, and k. Each C value defines an ellipse with its own y-axis length. The basic idea for the amount of screening is as follows: Two values C_{max} and C_{min} ($C_{max} > C_{min}$) are given, so that two ellipses with different length of the y axis can be defined. If a k atom is located outside of the larger ellipse defined by C_{max}—that is, if C value for a k atom is larger than C_{max}—it is assumed that the k atom does not give any effect on the i-j interaction. In this case, the screening factor is 1. If C value for a k atom is smaller than C_{min}, then it is assumed that the k atom completely screens the i-j interaction. In this case, the screening factor becomes zero. Between the two C values (C_{max} and C_{min}), the screening factor changes gradually. The resultant many-body screening function between atoms i and j is defined as the product of the screening factors due to all other neighbor atoms k. The screening function is then multiplied by the atomic electron densities and pair potential.

In the original 1NN MEAM,[3] $C_{max} = 2.8$ and $C_{min} = 2.0$ were chosen so that first nearest neighbors are completely

TABLE I. Parameters for the MEAM potential of Cu, Ag, Au, Ni, Pd, Pt, Al, and Pb. The units of the sublimation energy E_c, the equilibrium nearest-neighbor distance r_e, and the bulk modulus B are eV, Å, and 10^{12} dyn/cm^2, respectively.

	E_c	r_e	B	A	$\beta^{(0)}$	$\beta^{(1)}$	$\beta^{(2)}$	$\beta^{(3)}$	$t^{(1)}$	$t^{(2)}$	$t^{(3)}$	C_{max}	C_{min}	d
Cu	3.54	2.555	1.420	0.94	3.83	2.2	6.0	2.2	2.72	3.04	1.95	2.80	1.21	0.05
Ag	2.85	2.880	1.087	0.94	4.73	2.2	6.0	2.2	3.40	3.00	1.50	2.80	1.38	0.05
Au	3.93	2.880	1.803	1.00	5.77	2.2	6.0	2.2	2.90	1.64	2.00	2.80	1.53	0.05
Ni	4.45	2.490	1.876	0.94	2.56	1.5	6.0	1.5	3.10	1.80	4.36	2.80	0.81	0.05
Pd	3.91	2.750	1.955	0.94	5.15	2.2	6.0	2.2	4.50	1.47	4.85	2.80	1.69	0.05
Pt	5.77	2.770	2.884	0.90	4.92	2.2	6.0	2.2	3.94	−2.20	3.84	2.80	1.53	0.05
Al	3.36	2.860	0.794	1.16	3.20	2.6	6.0	2.6	3.05	0.51	7.75	2.80	0.49	0.05
Pb	2.04	3.500	0.488	1.01	5.42	2.2	6.0	2.2	3.10	3.91	1.25	2.80	0.81	0.00

unscreened for reasonably large thermal vibration in the fcc structure and the interactions are still first neighbor only even in the bcc structure. In the 2NN MEAM,[5,6] the second nearest-neighbor interactions are taken into consideration by giving a value smaller than 1.0 (2.0) to C_{min} for fcc (bcc) structure. In the 2NN MEAM, C_{min} is a material constant. However, if a value larger than 1.0 (2.0) is given to C_{min} for fcc (bcc) reference structure, then the screening function S becomes zero and the formalism of the 2NN MEAM becomes exactly the same as that of the 1NN MEAM. It has been shown[6] that the 2NN MEAM can be easily extended to describe binary alloy systems using a similar method as in the 1NN MEAM, and will not repeated here.

III. DETERMINATION OF THE PARAMETERS

The 2NN MEAM formalism for elements was applied to evaluate the MEAM parameters for the fcc elements Cu, Ag, Au, Ni, Pd, Pt, Al, and Pb. The parameters were determined by fitting to physical properties of each element, as will be described. The parameters finally determined for individual elements are listed in Table I. Here, the reference structure is fcc for all elements. In this section, the procedure for the determination of these parameter values are presented.

The 2NN MEAM formalism gives 14 model parameters as shown in Table I. Here, the values of the sublimation energy E_c, equilibrium nearest-neighbor distance r_e, and the bulk modulus B are given experimentally. Therefore, the actual number of adjustable parameters is eleven.

Of the 11 adjustable parameters (those listed in Table I except E_c, r_e, and B), C_{max} was given the same value (2.8) as in the 1NN MEAM.[3] For $\beta^{(1)}$, $\beta^{(2)}$, and $\beta^{(3)}$, it was also intended to keep the same values (2.2, 6.0, and 2.2, respectively) as in the 1NN MEAM because the effect of those parameters on the physical properties considered here was meager. In some cases, different values were given to $\beta^{(1)}$ and $\beta^{(3)}$ in order to better fit surface relaxation, as will be mentioned later again. In any case, the 1NN MEAM values (2.2, 6.0, 2.2) could be good starting values. By fixing the values of C_{max}, $\beta^{(1)}$, $\beta^{(2)}$, and $\beta^{(3)}$, the adjustable parameters whose values should be actually determined by fitting to physical properties become only seven, A, $\beta^{(0)}$, $t^{(1)}$, $t^{(2)}$, $t^{(3)}$, C_{min}, and d.

For the determination of the adjustable parameter values, a similar procedure to the previous one for bcc transition metals[6] was used. In the previous work, the $(\partial B/\partial P)$ value, elastic constants, surface energy, vacancy formation energy, and structural energy differences between fcc and bcc and between fcc and hcp have been used for the determination of the model parameter values. In the present work for the fcc metals, the (111) stacking fault energy, the activation energy of vacancy diffusion, and the thermal expansion coefficient were added to the fitting list. Also, special attention was paid to the surface reconstructions on the (100), (110), and (111) surfaces. This was because the original 1NN MEAM resulted in unexpected surface reconstructions for fcc elements.

The present authors were aware of the quasihexagonal reconstruction on (100) surfaces[12] and (1×2) missing row reconstruction on (110) surfaces[13] of the late $5d$ elements (Au and Pt in the present case). The quasihexagonal (100) surface reconstructions are reported to be not identical in all relevant elements, but qualitatively very similar to each other.[14] A representative (100) surface reconstruction obtained using the MEAM is shown in Fig. 1. This configuration was obtained after holding a thin film with (100) surface for several picoseconds at 800 K and cooling to 0 K. The problem in the original 1NN MEAM (with $C_{min}=2.0$) is that such a (100) reconstruction is obtained not only for Au and Pt, but also for all of the fcc metals considered. More seri-

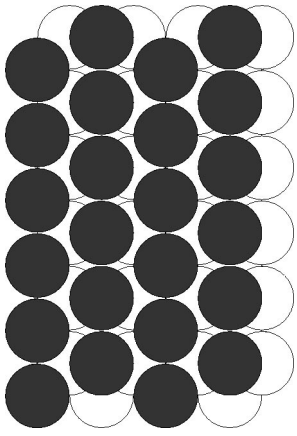

FIG. 1. Top view of the quasihexagonal reconstruction of the (100) surface frequently obtained using 1NN MEAM potentials for fcc elements.

TABLE II. $(\partial B/\partial P)$ at 0 K by first-principles calculation, at room temperature (RT) from experiments and MEAM value (0 K) obtained using $d=0$ and $d=0.05$ for individual elements. The FP calculation and experimental data are from Refs. 15 and 10, respectively.

	FP	Experimental	2NN MEAM	
	(0 K)	data (RT)	$d=0$	$d=0.05$
Cu	-	5.25	4.44	4.95
Ag	-	5.87	5.01	5.61
Au	-	5.90	5.40	6.06
Ni	4.89	-	4.39	4.90
Pd	-	-	5.28	5.93
Pt	-	-	5.33	5.98
Al	-	4.72	4.12	4.59
Pb	-	5.45	5.26	5.89

TABLE III. Effect of parameters on individual properties for fcc elements. The plus sign links individual parameters and relevant properties that can be used for determination of the parameter value.

	A	$\beta^{(0)}$	$t^{(1)}$	$t^{(2)}$	$t^{(3)}$	C_{min}
C_{11} and C_{12}		+				
C_{44}				+		
$E_{(surf)}$			+			
E_v^f			+			
Q^D			+			
E_{sf}					+	
$\Delta E_{bcc\rightarrow fcc}$	+					
$\Delta E_{fcc\rightarrow hcp}$	+				+	
ϵ						+
Surface reconstruction	+					+

ously, when similar MD runs were performed for thin films with (110) or (111) surfaces, even phase transitions as well as surface reconstructions resulted for most of the fcc elements. In an fcc structure with (111) surface, each atom on the surface layer should be located above three atoms of the next atomic layer. The representative (111) surface reconstruction obtained using the original 1NN MEAM was that each atom on the surface layer is located above two atoms of the next atomic layer instead of three. During the present work, it was confirmed by a first-principles calculation that such (111) surface reconstruction is a less stable one. Therefore, special attention was paid during the present work so that the abovementioned unexpected surface reconstructions and phase transitions can be avoided.

The procedure for determining the model parameter values begins with determining the value of d. This value could be determined separately from the other parameters and could be only determined by fitting the $(\partial B/\partial P)$ value. It has been decided in the previous study on bcc metals[6] to give either 0 or 0.05 to d according to the $(\partial B/\partial P)$ value by experiments or first-principles calculation. This was because the experimental information on $(\partial B/\partial P)$ was not always available and the accuracy of first-principles calculations was not very good to be used for the determination of the d value as a material constant. For Cu, Ag, Au, Al, and Pb, experimental information on $(\partial B/\partial P)$ was available while it was not for Ni, Pd, and Pt. The d values for Ni, Pd, and Pt were estimated based on first-principles calculation on Ni.[15] The first-principles (FP) calculated and experimentally reported $(\partial B/\partial P)$ values of individual elements are compared with the present MEAM values calculated for $d=0$ and $d=0.05$ in Table II. Based on this comparison, the finally selected d values are 0 for Pb and 0.05 for all others.

After the d value is determined, all the other model parameters A, $\beta^{(0)}$, $t^{(1)}$, $t^{(2)}$, $t^{(3)}$, and C_{min} are determined fitting elastic constants (C_{11}, C_{12}, C_{44}), surface energy $(E_{(surf)})$, vacancy formation energy (E_v^f), activation energy of vacancy diffusion (Q), (111) stacking fault energy (E_{sf}), structural energy differences $(\Delta E_{fcc\rightarrow bcc}, \Delta E_{fcc\rightarrow hcp})$, thermal expansion coefficient (ϵ), and examining the occurrence of surface reconstructions. Generally, the effect of each parameter on individual properties is complicated, and it is impossible to relate one property to one parameter. However, the effects of some parameters are certainly confined to only few properties, and the evaluation of parameters can be done systematically. Table III shows which parameters can be determined by fitting which properties for the fcc elements. Here, the properties that can be used for determining each parameter value are linked by the plus sign. The plus sign does not mean that the individual properties are affected only by the linked parameter values. For example, the A parameter has an effect on almost all properties. However, the surface energies or the vacancy formation energy are not fitted by adjusting the A value because they can be fitted adjusting other parameters.

In the present work, it was found that the phase transition that occurred during MD runs of thin films at finite temperatures could be removed by lowering the C_{min} values. In a previous study,[9] it has also been found that the thermal expansion is strongly affected by the C_{min} value, being larger as a smaller C_{min} value is given. Here, in the present study, it was confirmed that the observation holds for all elements considered. Therefore, a smaller C_{min} value than the corresponding 1NN MEAM value (2.0) was given as an initial value, confirming that the given C_{min} value does not result in unexpected phase transitions. However, the (111) surface reconstruction and especially the (100) surface reconstruction were not controlled by adjusting the C_{min} value. These unexpected surface reconstructions could only be removed by adjusting the A values. Therefore an A value which is closest to the previous 1NN value but does not result in unexpected surface reconstructions was selected for each element. For a given set of C_{min} and A values the elastic constants C_{11} and C_{12} could only be fitted by adjusting the $\beta^{(0)}$ parameter. Then the other elastic constant C_{44} was fitted by adjusting the $t^{(2)}$ parameter. The (111) stacking fault energy could only be effectively fitted by adjusting the $t^{(3)}$ value and, therefore, was used to determine the $t^{(3)}$ value. Finally, the value of $t^{(1)}$ was optimized so that the (100), (110), and (111) surface energies, vacancy formation energy, and activation energy of vacancy diffusion are reproduced equally well. This proce-

TABLE IV. Calculated and experimental elastic constants (10^{12}dyn/cm^2). Experimental data are from Ref. 16.

	C_{11}		C_{12}		C_{44}	
	MEAM	Expt.	MEAM	Expt.	MEAM	Expt.
Cu	1.762	1.762	1.249	1.249	0.818	0.818
Ag	1.315	1.315	0.973	0.973	0.511	0.511
Au	2.015	2.016	1.697	1.697	0.454	0.454
Ni	2.612	2.612	1.508	1.508	1.317	1.317
Pd	2.342	2.341	1.761	1.761	0.712	0.712
Pt	3.581	3.580	2.535	2.536	0.775	0.774
Al	1.143	1.143	0.619	0.619	0.316	0.316
Pb	0.556	0.555	0.454	0.454	0.194	0.194

dure was repeated changing C_{min} value fitting the thermal expansion coefficient.

Using the above procedure, it was usually possible to exactly reproduce the target value of each specific property. However, it was generally impossible to reproduce target values of all properties, simultaneously. Among all properties considered, it was believed that the elastic constants are those most accurately measured. Therefore, the determination of parameters was done so that the elastic constants are exactly reproduced and so that the other property values are reasonably reproduced considering their accuracy. In the previous study for bcc elements,[6] A and $t^{(3)}$ values were determined mainly fitting the structural energy difference between fcc and bcc and between fcc and hcp structures, respectively. This was possible because at that time unexpected surface reconstructions were not a problem and the (111) stacking fault energy was not considered. In the present study, the structural energy differences were not the main target of fitting. Instead, it was only checked during the optimization procedure that the predicted values are not far from the target values.

IV. CALCULATION OF PHYSICAL PROPERTIES

The potentials determined by the above procedure will now be used to compute various physical properties of individual elements in order to evaluate the reliability of them. The calculations were performed on bulk properties (elastic constants, structural energy differences), point defect properties (vacancy and interstitial formation energy and formation volume, activation energy of vacancy diffusion), planar defect properties (stacking fault energy, surface energy, surface relaxation and reconstruction) and thermal properties (thermal expansion coefficients, specific heat, melting point, heat of melting). In this section, some comparisons between the present calculation and experimental data or high level calculation will be presented.

Table IV shows the calculated and experimental elastic constants (C_{11}, C_{12}, and C_{44}) for individual elements. The elastic constants were given highest weight during the fitting procedure and could be reproduced almost exactly.

The calculated structural energy difference and volume of various crystal structures are listed in Table V. Though the energy differences between fcc and bcc ($\Delta E_{fcc\rightarrow bcc}$) and between fcc and hcp ($\Delta E_{fcc\rightarrow hcp}$) were included in the fitting procedure, no actual action was made to fit these values. It was only checked that the predicted values are not far from the target values. The experimental data being compared to the computed $\Delta E_{fcc\rightarrow bcc}$ and $\Delta E_{fcc\rightarrow hcp}$ are thermodynamically assessed values using the calphad method.[17] It is shown that the $9R$ structure which is reported to occur during the bcc $\rightarrow$ fcc transition of Cu precipitates in the bcc Fe matrix[18–20] is the next stable structure of the fcc elements considered.

The next property looked at was point defects. Besides the vacancy formation energy and the activation energy of vacancy diffusion (vacancy formation energy + vacancy migration energy), which were used for fitting, the formation energy and structure of a self-interstitial and the volume change due to the formation of a vacancy or self-interstitial were calculated and are compared with available experimental information in Table VI. According to the present calculation, the most stable form of a self-interstitial is a dumbbell along [100] direction, in agreement with experimental information.[21]

The surface properties (surface energy and its anisotropy, relaxation, and reconstruction) are important for an atomic scale simulation on thin-film processes and also a good test-

TABLE V. Calculated structural energy differences ΔE(eV) and atomic volumes v/n(Å^3). The energy differences are relative to fcc. The atomic volume of fcc and experimental data for the fcc→bcc and fcc→hcp energy differences are also presented for comparison.

	fcc	bcc			hcp				$9R$		Simple cubic		Diamond	
	v/n	$\Delta E_{fcc\rightarrow bcc}$	Expt. [a]	v/n	$\Delta E_{fcc\rightarrow hcp}$	Expt. [a]	c/a	v/n	$\Delta E_{fcc\rightarrow 9R}$	v/n	$\Delta E_{fcc\rightarrow sc}$	v/n	$\Delta E_{fcc\rightarrow dia}$	v/n
Cu	11.79	0.08	0.04	11.59	0.007	0.006	1.64	11.81	0.005	11.80	0.41	13.03	0.90	18.58
Ag	16.89	0.08	0.04	16.51	0.005	0.003	1.64	16.90	0.003	16.90	0.31	19.08	0.66	26.96
Au	16.89	0.06	0.04	16.18	0.009	0.003	1.65	16.90	0.006	16.90	0.22	18.67	0.67	26.05
Ni	10.92	0.16	0.09	10.91	0.02	0.01	1.65	10.93	0.014	10.93	0.66	13.06	1.42	20.03
Pd	14.71	0.17	0.11	14.10	0.02	0.02	1.65	14.73	0.013	14.72	0.41	16.78	1.11	24.89
Pt	15.03	0.28	0.16	14.72	0.02	0.03	1.65	15.05	0.015	15.04	0.76	17.55	1.71	25.97
Al	16.54	0.12	0.10	16.80	0.03	0.06	1.69	16.66	0.02	16.62	0.13	17.60	0.95	31.24
Pb	30.32	0.04	0.02	30.27	0.003	0.003	1.64	30.33	0.002	30.33	0.11	32.79	0.30	44.28

[a]Thermodynamically assessed values (room-temperature data) (Ref. 17).

TABLE VI. Calculated point defect properties. Values listed are the relaxed vacancy formation energy E_v^f(eV), activation energy of vacancy diffusion Q(eV), vacancy formation volume ΔV_v^f, and relaxed formation energy E_I^f(eV), structure, and formation volume ΔV_I^f of the most stable interstitial. The experimental information on the vacancy formation energies, activation energies of diffusion and on the vacancy or interstitial formation volume are also presented for comparison. Here Ω is the equilibrium atomic volume.

	E_v^f		Q		$\Delta V_v^f/\Omega$		Interstitial		$\Delta V_I^f/\Omega$	
	MEAM	Expt.	MEAM	Expt.	MEAM	Expt.	E_I^f	Structure	MEAM	Expt.
Cu	1.11	1.03 [a],1.19 [b],1.30 [c]	2.19	2.09 [a]	−0.25	−0.22 [d]	3.05	[100] dumbbell	1.72	1.45 [d]
Ag	0.94	1.1 [c]	1.86	1.77 [e]	−0.26	−0.06 [f]	2.86	[100] dumbbell	1.87	
Au	0.90	0.9 [c]	1.75	1.70 [e]	−0.36	−0.55 [f]	2.93	[100] dumbbell	1.77	
Ni	1.51	1.6 [g]	2.98	2.87 [e]	−0.14	−0.3 [h]	4.88	[100] dumbbell	1.90	1.70 [h]
Pd	1.50	1.4 [i],1.7 [j]	2.71	2.76 [e]	−0.27		4.68	[100] dumbbell	1.89	
Pt	1.50	1.35 [j],1.5 [c]	2.70	2.64 [e]	−0.34		6.64	[100] dumbbell	1.94	
Al	0.68	0.68 [k]	1.33	1.28 [e]	−0.28		2.49	[100] dumbbell	1.70	
Pb	0.58	0.58	1.16	1.11 [e]	−0.29		1.54	[100] dumbbell	1.70	

[a]Reference 22.
[b]Reference 23.
[c]Reference 24.
[d]Reference 25.
[e]Reference 26.
[f]Reference 27.
[g]Reference 28
[h]Reference 29.
[i]Reference 30.
[j]Reference 31.
[k]Reference 32.

bed where the reliability of an empirical potential can be evaluated. Actually the surface properties, especially the reconstruction of the (100) or (110) surface, were one of the main reasons of the present study for a redetermination of MEAM parameters for the fcc elements, because the original 1NN MEAM parameters resulted in unexpected surface reconstructions as mentioned earlier. The surface energies and the surface relaxations of the three low-index surfaces, (100), (110), and (111) as well as the relaxed (111) stacking fault energy are presented in Table VII, in comparison with experimental information. The experimental surface energy values E_{poly}^{expt} are for polycrystalline solids. All these are extrapolated values from high-temperature experimental data through some modeling approaches on the temperature dependences of the surface energy.[34,38] The calculated stacking fault energies using the present MEAM potentials are reasonable while the calculated surface energies are generally lower than experimental data. In the case of surface relaxation, the scattering in experimental data is generally large, and the present calculation shows reasonable values within experimental uncertainties.

In Table VII, the relative stabilities of the quasihexagonal reconstruction of the (100) surface and the (1×2) missing row reconstruction of the (110) surface to corresponding (1×1) unreconstructed surfaces are also given by ''O'' and ''X.'' ''O'' means that the relevant reconstructed surface is more stable than the (1×1) unreconstructed surface. Experimentally, it is reported that the quasihexagonal (100) surface reconstruction and (1×2) missing row (110) surface reconstruction occur only on Au and Pt surfaces among the fcc elements considered. The present potential correctly predicts that such reconstructions are stable on both (100) and (110) surfaces of Pt. However, for Au, both reconstructions are not predicted to be stable. Further, the (1×2) missing row surface reconstruction is incorrectly predicted to be stable on (110) surfaces of Ni and Al. It should be noted here that the results in Table VII do not mean that the MEAM formalism describes the (100) surface properties better than (110) surface properties for fcc elements. For example, for Ni, it was possible to adjust the parameters so that (110) surface reconstruction is correctly described, losing a correct description of the (100) surface reconstruction. During the present work, it was found that the (100) surface reconstruction is obtained easily by MD runs at finite temperatures, while the (110) missing row reconstruction is not. The unexpected (100) surface reconstruction had to be avoided in order to apply the MEAM potential to any atomistic simulation on thin-film processes on the (100) surfaces. For this practical purpose, when the surface reconstructions of (100) and (110) surfaces are not correctly reproduced simultaneously, the adjustment of the parameters was made in a way to describe the (100) surface reconstruction correctly.

Finally, the properties calculated using the present MEAM potential are the thermal properties such as thermal expansion coefficient, specific heat, melting point, heat of melting, and volume change on melting. The results are compared with available experimental data in Table VIII. The calculated thermal expansion coefficients are in excellent agreement with experimental data because these values were included in the fitting procedure. The melting points are those calculated using a interface velocity method. The heat of melting is the value obtained at the calculated melting point of each element. The calculated heat of melting and volume change of melting are generally larger than the relevant experimental data.

As can be seen in Tables IV–VIII, the present MEAM

TABLE VII. Calculated stacking fault energies E_{sf} (erg/cm^2), surface energies $E_{(surf)}$ (erg/cm^2), and relaxations Δd_{12} (%) of the low-index surfaces. Relative stabilities of hexagonal (100) and (1×2) missing row (110) reconstructions to relevant unreconstructed (1×1) surfaces are also given by "O" or "X," where "O" means that the corresponding reconstruction is energetically favorable. Δd_{12} means the change of interlayer spacing between the first and second surface layers, relative to corresponding bulk spacing. The experimental surface energy values E_{poly}^{expt} are for polycrystalline solids and are those extrapolated from high-temperature experimental data. Values in the second row for each element are experimental or high-level calculation data for corresponding stacking fault energy, surface relaxation, and surface reconstruction. Experimental data for surface relaxations are from compilation by Wan *et al.* (Ref. 33) if not specifically designated.

			(100)			(110)			(111)	
	E_{sf}	E_{poly}^{expt}	$E_{(100)}$	Δd_{12}	Recon.	$E_{(110)}$	Δd_{12}	Recon.	$E_{(111)}$	Δd_{12}
Cu	42	1770 [a]	1382	-2.5	X	1451	-9.3	X	1185	-3.1
	<78 [b]			-1.1 ± 0.4, -2.1	X		-5.3 ± 2.4, -10.0 ± 2.5	X		>0, -0.7 ± 0.5
Ag	21	1320 [a]	983	-2.4	X	1010	-10.4	X	842	-2.1
	<22 [b]			0 ± 1.5, -1.9 [f]	X		-7.8 ± 2.5, -11.0, -7.0 [g]	X		0.0 ± 2
Au	40	1540 [a]	1138	-4.3	X	1179	-17.5	X	928	-2.7
	<55 [b]			-1.0 [f]	O		-9.8 [g]	O		
Ni	125	2240 [a]	1943	-1.3	X	2057	-6.0	O	1606	-1.4
	125 [c]			1.1 ± 1.1, -3.2 ± 0.5	X		-4.8 ± 1.7, -9.8 ± 1.8	X		-1.2 ± 1.2
Pd	100	2043 [d]	1743	-0.8	X	1786	-11.2	X	1435	-0.3
	100 [c]			0.3 ± 2.6, [h] -0.8 [f]	X		-6.0 ± 2.0	X		0.0 ± 4.4, [h] -0.9 ± 1.3 [h]
Pt	110	2691 [d]	2288	-0.8	O	2328	-16.0	O	1710	$+2.6$
	110 [c]			0.0 ± 5.1, [h] 0.0 [f]	O		-14 [i]	O		1.1 ± 4.4, [h] 1.5 ± 1.0
Al	141	1085 [d]	848	$+1.8$	X	948	-8.9	O	629	$+1.0$
	<166 [b, e]			$+1.8$	X		-8.5 ± 1.0	X		0.9 ± 0.5, 2.2
Pb	9	534 [d]	426	-4.2	X	440	-13.2	X	375	-4.6
	-			-8.0 ± 1.2	X		-15.8 ± 2.5	X		

[a]Reference 34.
[b]References 35–37.
[c]Reference 37.
[d]Reference 38.
[e]References 39, 40.
[f]Reference 14.
[g]Reference 41.
[h]Reference 42.
[i]Reference 43

potentials reproduce the physical properties of the fcc elements fairly well. Generally, the calculated bulk properties (elastic properties and structural energy) and the point defect properties are quite good. Though the calculated surface energies are slightly lower than experimental data, the order in size of surface energy among elements is kept in agreement with experimental information. The calculated amount of surface relaxation is thought to be reasonable when compared to experimental information with large scattering. The potential problem is that the quasihexagonal (100) reconstruction and the (1×2) missing row (110) reconstruction are incorrectly predicted for some elements [Au in the case of (100) and Au, Ni, and Al in the case of the (110) surface]. This should be the subject of future study for further devel-

TABLE VIII. Calculated thermal properties. Values listed are the thermal expansion coefficient ϵ (10^{-6}/K), specific heat C_p(J/mol K), melting point (K), heat of melting ΔH_m(kJ/mol), and volume change on melting $\Delta V_m/V_{solid}$ (%). The experimental data for thermal expansion coefficient, specific heat, and volume change are from Ref. 26 and others are from Ref. 17.

	ϵ (0–100 °C)		C_p (0–100 °C)		Melting point		ΔH_m		$\Delta V_m/V_{solid}$	
	MEAM	Expt.	MEAM	Expt.	MEAM	Expt.	MEAM	Expt.	MEAM	Expt.
Cu	17.0	17.0	24.9	24.5	1602	1358	18.6	13.3	7.7	4.2
Ag	18.9	19.1	24.6	25.2	1346	1235	17.8	11.3	9.2	3.8
Au	14.2	14.1	24.0	25.6	1410	1337	17.8	12.5	7.4	5.1
Ni	12.6	13.3	25.4	26.5	2013	1728	24.6	17.5	9.1	4.5
Pd	11.1	11.0	23.6	26.3	2014	1828	35.6	16.7	12.8	-
Pt	9.2	9.0	24.6	26.2	2374	2042	33.2	22.2	9.0	-
Al	22.0	23.5	26.2	24.7	937	933	11.0	10.7	6.7	6.5
Pb	30.1	29.0	26.3	26.9	705	601	7.0	4.8	5.7	3.5

opment of the MEAM formalism. The reason for the calculation of thermal properties is two. One is of course to see whether the present potentials result in melting behavior of the elements correctly. The other is to confirm that the fcc structure is the most stable structure up to the melting temperature for all elements considered. Important here is that the problems in the original 1NN MEAM descriptions of the fcc elements—the instability of fcc structure and incorrect occurrence of surface reconstructions or structural transitions during MD runs as well as the low thermal expansion coefficient—are mostly solved.

All the present calculations are performed using a radial cutoff distance for each element. These are 4.0 Å for Ni and Cu, 5.5 Å for Pb, and 4.5 Å for the others. The results of the present calculations are independent from radial cutoff distances, as far as they are larger than the second nearest-neighbor distance by more than about 0.2 Å. This is because of the many-body screening. The recommended value is the mean value between the second and third nearest-neighbor distances.

During the present study, great effort has been made to solve the already-mentioned problems of the 1NN MEAM potentials on the fcc elements. Using the 1NN MEAM parameters as a starting set, the effects of individual parameters on the various properties were carefully examined. The instability of fcc structure that occurred for 1NN MEAM Al and the structural transitions that occurred for most of the fcc elements considered during MD runs over thin films with (110) and/or (111) surfaces at finite temperatures could be solved by giving lower values to C_{min} than the 1NN MEAM value 2.0. However, the occurrence of the already-mentioned unexpected surface reconstructions on (100) and (111) surfaces could not be avoided by simply lowering the C_{min} value. These surface reconstructions, especially the hexagonal-type (100) surface reconstruction (Fig. 1) that occurred for all elements considered, could only be removed by changing the value of A significantly from the initial 1NN MEAM values.

For Cu, Ag, Ni, and Pd, the A value had to be lowered compared to corresponding 1NN MEAM values. This made the (110) reconstruction more stable for Ni even though the energy difference is small. According to the original 1NN MEAM of Ni, the reconstructed (110) surface was less stable than the unreconstructed surface. Instead, the reconstructed (100) surface was much more stable than the unreconstructed surface. With the present description of Ni, the situation is the opposite. The selection of a low-A value for Ni in the present study is only due to a practical reason as already mentioned—that is, in order to make the (100) reconstruction that occurs easily during MD runs at finite temperatures less stable than the corresponding unreconstructed surface structure. For Au and Pt, the (100) reconstructions were the expected ones. However, for these elements the (111) reconstruction mentioned in the previous section became a problem. The A parameter values had to be lowered in order to remove the unexpected (111) surface reconstructions. For Au, more attention was paid to avoid the unexpected (111) surface reconstruction rather than to reproduce the (100) reconstruction. In the case of Al, the problem was that the (1 $\times$2) missing row reconstruction on the (110) surface is too much stable compared to unreconstructed surface. This could be improved a little by increasing the A parameter value. However, the incorrect (110) reconstruction could not be completely removed by adjusting parameter values within the framework of current formalism of the MEAM. It should be mentioned here that an attempt to improve the reconstruction properties by changing the $\beta^{(1)}$, $\beta^{(2)}$, and $\beta^{(3)}$ values has been also made during the present work. However, this attempt was not successful. For Pb, the energy difference between the reconstructed and unreconstructed (100) surfaces according to the original 1NN MEAM was small. The (100) reconstruction could be made less stable than the corresponding unreconstructed surface structure easily by adjusting the parameter values other than the A parameter. The main difference between the 1NN MEAM and the present 2NN MEAM potential for Pb is that the C_{min} parameter was given a value of 0.81 in the present potential instead of the 1NN value 2.0. With the 1NN MEAM potential the calculated thermal expansion coefficient in the temperature range of 0–100 °C was about 3×10^{-6} K^{-1}. According to the present description it is 30×10^{-6} K^{-1}. The corresponding experimental data is 29×10^{-6} K^{-1}.

In the present study, for Ni and Al the $\beta^{(1)}$ and $\beta^{(3)}$ parameters were given different values from the initial 1NN MEAM value of 2.2. By this the surface relaxations could be predicted in better agreement with experimental information. However, this adjustment was not extended to other elements because the agreements were already good or the experimental information was not decisive and also because such an extension was not helpful to improve the surface reconstruction properties. It should be mentioned here that recently Van Beurden and Kramer[44] presented new 1NN MEAM parameter sets for Rh, Pd, Ir, and Pt. They utilized all the $\beta^{(1)}$, $\beta^{(2)}$, and $\beta^{(3)}$ parameters as adjustable parameters instead of giving them fixed values as in the original MEAM (Ref. 3) and in the present work. Using the new parameter sets, they could describe the surface relaxation and reconstruction properties correctly even though the description of elastic properties (C_{11}, C_{12}, and C_{44}) was not very good. This means that the possibility of giving nonfixed values to $\beta^{(1)}$, $\beta^{(2)}$, and $\beta^{(3)}$ should not be closed in a future study especially to improve the surface reconstruction properties.

As already mentioned, the flexibility of the present MEAM formalism is that there exist no clear boundary between the 1NN MEAM and the 2NN MEAM. The 2NN MEAM formalism becomes exactly the same as that of 1NN MEAM if the C_{min} parameter is adjusted so that only first nearest-neighbor interactions are involved in the calculation of background electron density for a reference structure $\overline{\rho}^0$ and pair potential $\rho(R)$. The boundary value of C_{min} that categorizes the formalism into 1NN or 2NN MEAM is about 1.0 in the case of fcc reference structure. Therefore, one can say that in the present study Ni, Al, and Pb were described by the 2NN MEAM while the other elements were described by the 1NN MEAM. The main difference between the present potentials and the originally published 1NN MEAM potentials[3] for the fcc elements is not that the 2NN MEAM

formalism is adapted in the present study. A more important finding in the present study is that the degree of many-body screening should be a material property, giving different values to C_{min} of individual elements. Actually, a similar treatment has been done in the previous study on bcc transition metals.[6] For a bcc structure, the formalism becomes 2NN if a value lower than 2.0 (1NN MEAM value) is given to C_{min}, and such low values were indeed given for all the bcc elements considered. At that time, it was thought that considering second nearest-neighbor interactions is important because the second nearest-neighbor distance in the bcc structure is greater than that of the first nearest-neighbor distance by only 15%. In the present case for fcc elements, even though the 2NN MEAM is applied to some elements, the portion of second nearest-neighbor interactions that is included in the energy calculation is less than a few percent. Actually, the S value in Eqs. (12)–(15) is only about 0.025 for Al, the element with the lowest C_{min} value. The calculated 0 K bulk properties and point defect properties are not affected by the C_{min} parameter if this value is greater than 1.0. The fact that lower values of C_{min} than 2.0 but larger than 1.0 were needed for many fcc elements even though they would not give significant effect on the 0 K bulk properties indicates that generally many-body screening gives decisive effects on the surface and thermal properties where the degree of defect is relatively severe. For a better description of surface and thermal properties, the future study on the MEAM formalism should be concentrated on the functional form of many-body screening which was actually developed in an *ad hoc* manner.[3] It should be mentioned here that a different form[9] of Eq. (4) has been also tested during the present study and was found to yield a marginal but a certain difference. The present study also shows the importance of thermal properties (including structural stability) as a member of test bed for semiempirical potentials.

Further, it should be noted here that the process of finding the fitting parameters was kept relatively simple in the present study, because a more extensive method (a simultaneous fit, one involving all parameters) would be computationally very costly. As a result, the agreement of calculated material properties with experimental material properties, both fitted and unfitted, was not necessarily optimal. Conditions relatively far away from equilibrium were not tested extensively, so that applying the potentials in such cases should be done only with extreme caution. Also, as already shown, though the need for including second neighbors in modeling fcc elements was investigated in this paper, the outcome is not conclusive. The reason for this is that all screening factors for second neighbors are 0.025 or smaller. An alternative first-neighbors-only description with different parameters may be equally well possible. The current results constitute just one of the possibilities at the indicated level of compatibility with the fitted experimental data.

Finally it should be mentioned that the structural stability problem in the 1NN MEAM for hcp elements[4] found by Mae *et al.*[7] may be solved by similar treatments to the present study. The present authors could confirm that the structural instability[7] of hcp Ti according to the 1NN MEAM (Ref. 4) could be solved by simply lowering the C_{min} value from 2.0 to 0.81. An extensive study to improve the MEAM for hcp elements will be performed near future.

V. CONCLUSIONS

The problems caused by the original first nearest-neighbor MEAM potentials for fcc elements, the structural instability, the phase transitions, or incorrect surface reconstructions on thin films with (100), (110), and/or (111) surfaces and the too low thermal expansion coefficients have now been mostly solved. The MEAM parameter values for Cu, Ag, Au, Ni, Pd, Pt, Al, and Pb were redetermined, adapting a recently developed second nearest-neighbor MEAM formalism as well as the original first nearest-neighbor MEAM. The new MEAM potentials yield the bulk properties, point defect properties, planar defect properties, and thermal properties of the fcc elements considered in good agreement with experimental information. The present study shows that in the MEAM the degree of many-body screening should be a material property, giving different values to C_{min} of individual elements, and that thermal properties, especially the structural stability, should be included as a checkpoint during the development of semiempirical potentials.

ACKNOWLEDGMENTS

This work has been financially supported by the Ministry of Science and Technology of Korea through the National R&D Project for Nano Science and Technology (Grant No. M1-0213-04-0002) and by the U.S. Department of Energy, Office of Basic Energy Sciences (M.I.B.).

*FAX: +82-54-279-2399.
Electronic address: calphad @postech.ac.kr
†FAX: 505-667-8021. Electronic address: baskes@lanl.gov

[1] M.I. Baskes, Phys. Rev. Lett. **59**, 2666 (1987).
[2] M.I. Baskes, J.S. Nelson, and A.F. Wright, Phys. Rev. B **40**, 6085 (1989).
[3] M.I. Baskes, Phys. Rev. B **46**, 2727 (1992).
[4] M.I. Baskes and R.A. Johnson, Modell. Simul. Mater. Sci. Eng. **2**, 147 (1994).
[5] B.-J. Lee and M.I. Baskes, Phys. Rev. B **62**, 8564 (2000).
[6] B.-J. Lee, M.I. Baskes, H. Kim, and Y.K. Cho, Phys. Rev. B **64**, 184102 (2001).
[7] K. Mae, T. Nobata, H. Ishida, S. Motoyama, and Y. Hiwatari, Modell. Simul. Mater. Sci. Eng. **10**, 205 (2002).
[8] M.I. Baskes, Mater. Sci. Eng., A **261**, 165 (1999).
[9] M.I. Baskes, Mater. Chem. Phys. **50**, 152 (1997).
[10] J.H. Rose, J.R. Smith, F. Guinea, and J. Ferrante, Phys. Rev. B **29**, 2963 (1984).
[11] M.I. Baskes, J.E. Angelo, and C.L. Bisson, Modell. Simul. Mater. Sci. Eng. **2**, 505 (1994).
[12] S. Hagstrom, H.B. Lyon, and G. Samorjai, Phys. Rev. Lett. **15**, 491 (1965).
[13] I.K. Robinson, Phys. Rev. Lett. **50**, 1145 (1983).
[14] V. Fiorentini, M. Methfessel, and M. Scheffler, Phys. Rev. Lett.

71, 1051 (1993).
[15] Hanchul Kim (private communication).
[16] G. Simmons and H. Wang, *Single Crystal Elastic Constants and Calculated Aggregate Properties*: *A Handbook*, 2nd ed. (MIT Press, Cambridge, MA, 1971).
[17] A.T. Dinsdale, CALPHAD: Comput. Coupling Phase Diagrams Thermochem. **15**, 317 (1991).
[18] S. Pizzini, K.J. Robert, W.J. Phythian, C.A. English, and G.N. Greaves, Philos. Mag. Lett. **61**, 223 (1990).
[19] H.A. Hardouin Duparc, R.C. Doole, M.L. Jenkins, and A. Barbu, Philos. Mag. A **71**, 325 (1995).
[20] P.J. Othen, M.L. Jenkins, and G.D.W. Smith, Philos. Mag. A **73**, 249 (1996).
[21] P. Ehrhart, J. Nucl. Mater. **69/70**, 200 (1978).
[22] W. Schüle, Z. Metallkd. **89**, 672 (1998).
[23] Th. Hehenkamp, W. Berger, J.-E. Kluin, Ch. Lüdecke, and J. Wolff, Phys. Rev. B **45**, 1998 (1992).
[24] R.W. Balluffi, J. Nucl. Mater. **69/70**, 240 (1978).
[25] P. Ehrhart, J. Nucl. Mater. **69/70**, 200 (1978).
[26] *Smithells Metals Reference Book*, 7th ed., edited by E.A. Brandes and G.B. Brook (Butterworth-Heinemann, Oxford, 1992).
[27] P. Ehrhart, in *Vacancies and Interstitials in Metals*, edited by A. Seeger, D. Schumacher, W. Schilling, and J. Diehl (North-Holland, Amsterdam, 1970), p. 363.
[28] W. Wycisk and M. Feller-Kniepmeier, J. Nucl. Mater. **69/70**, 616 (1978).
[29] O. Bender and P. Ehrhart, in *Point Defects and Defect Interactions in Metals*, edited by J. Takamura, M. Doyama, and M. Kiritani (North-Holland, Amsterdam, 1982), p. 639.
[30] S.M. Foiles, M.I. Baskes, and M.S. Daw, Phys. Rev. B **33**, 7983 (1986).
[31] H. Schultz and P. Ehrhart, in *Atomic Defects in Metals*, edited by H. Ullmaier, Landolt-Börnstein, New Series, Group III (Springer, Berlin, 1991).
[32] H.-E. Schaefer, R. Gugelmeier, M. Schmolz, and A. Seeger, Mater. Sci. Forum **15-18**, 111 (1987).
[33] J. Wan, Y.L. Fan, D.W. Gong, S.G. Shen, and X.Q. Fan, Modell. Simul. Mater. Sci. Eng. **7**, 189 (1999).
[34] W.R. Tyson and W.A. Miller, Surf. Sci. **62**, 267 (1977).
[35] L.E. Murr, *Interfacial Phenomena in Metals and Alloys* (Addison-Wesley, Reading, MA, 1975).
[36] J.P. Hirth and J. Lothe, *Theory of Dislocations* (Wiley-Interscience, New York, 1982).
[37] C.S. Barrett and T.B. Massalski, *Structure of Metals* (McGraw-Hill, New York, 1966).
[38] L.Z. Mezey and J. Giber, Jpn. J. Appl. Phys., Part 1 **21**, 1569 (1982).
[39] R.H. Rautioaho, Phys. Status Solidi B **112**, 83 (1982).
[40] K.H. Westmacott and R.L. Peck, Philos. Mag. **23**, 611 (1971).
[41] K.-P. Bohnen and K.M. Ho, Electrochim. Acta **40**, 129 (1995).
[42] P.R. Watson, M.A. Van Hove, and K. Hermann, *Atlas of Surface Structures: Based on the NIST Surface Structure Database* (*SSD*) (American Chemical Society, Washington, D.C., 1994), Vol. 1A.
[43] S.J. Jenkins, M.A. Petersen, and D.A. King, Surf. Sci. **494**, 159 (2001).
[44] P. van Beurden and G.J. Kramer, Phys. Rev. B **63**, 165106 (2001).